BBA - Bioenergetics 1864 (2023) 148958

Contents lists available at ScienceDirect

BBA - Bioenergetics

journal homepage: www.elsevier.com/locate/bbabio

The protein family of pyruvate:quinone oxidoreductases: Amino acid sequence conservation and taxonomic distribution

Filipe M. Sousa, Bárbara Fernandes, Manuela M. Pereira *

Instituto de Tecnologia Química e Biológica-António Xavier, Universidade Nova de Lisboa, Av. da República EAN, 2780-157 Oeiras, Portugal
BioISI–Biosystems & Integrative Sciences Institute and Department of Chemistry and Biochemistry, Faculty of Sciences, University of Lisboa, 1749-016 Lisboa, Portugal

ARTICLE INFO

Keywords:
Respiratory chain
Monotopic quinone reductases
Flavoproteins
Thiamine pyrophosphate
Taxonomic profile
Amino-acid residue conservation
Pyruvate metabolism

ABSTRACT

Pyruvate:quinone oxidoreductases (PQOs) catalyse the oxidative decarboxylation of pyruvate to acetate and concomitant reduction of quinone to quinol with the release of CO_2. They are thiamine pyrophosphate (TPP) and flavin-adenine dinucleotide (FAD) containing enzymes, which interact with the membrane in a monotopic way. PQOs are considered as part of alternatives to most recognized pyruvate catabolizing pathways, and little is known about their taxonomic distribution and structural/functional relationship.

In this bioinformatics work we tackled these gaps in PQO knowledge. We used the KEGG database to identify PQO coding genes, performed a multiple sequence analysis which allowed us to study the amino acid conservation on these enzymes, and looked at their possible cellular function. We observed that PQOS are enzymes exclusively present in prokaryotes with most of the sequences identified in bacteria. Regarding the amino acid sequence conservation, we found that 75 amino acid residues (out of 570, on average) have a conservation over 90 %, and that the most conserved regions in the protein are observed around the TPP and FAD binding sites. We systematized the presence of conserved features involved in Mg^{2+}, TPP and FAD binding, as well as residues directly linked to the catalytic mechanism. We also established the presence of a new motif named "HEH lock", possibly involved in the dimerization process. The results here obtained for the PQO protein family contribute to a better understanding of the biochemistry of these respiratory enzymes.

1. Introduction

Thiamine pyrophosphate (TPP) containing enzymes are a taxonomically widespread group of proteins, which take part in a multitude of metabolic reactions. Based on their reactions, TPP containing enzymes have been classified into five super families [1]. The largest of these families is composed of decarboxylases acting on oxo-acids. Among these enzymes are for example acetohydroxyacid synthases, benzaldehyde aldolases, pyruvate decarboxylases, oxalyl-CoA decarboxylases, indolepyruvate decarboxylases and the only oxidoreductases of this super-family the pyruvate oxidases. Pyruvate oxidases can be further divided into the soluble pyruvate:oxygen oxidoreductases (POX) and the membrane bound pyruvate:quinone oxidoreductases (PQO). PQOs catalyse the oxidative decarboxylation of pyruvate to acetate and carbon dioxide, using a liposoluble quinone as a physiological electron acceptor [2–4].

They are peripheral membrane proteins bound to the cytoplasmatic side of the membrane consisting of four identical subunits. Each subunit, with a molecular mass of approximately 60 kDa, has a tightly bound FAD and requires TPP and Mg^{2+} for the catalytic activity. Four domains are recognized in each monomer (Fig. 1, panel A): (i) the pyrimidine binding domain (magenta); (ii) the FAD binding domain (yellow); (iii) the pyrophosphate binding domain (orange); and (iv) the C-terminal domain through which the membrane binding occurs (blue) [5,6]. As a quinone reducing enzyme, PQO may be considered as part of the respiratory chain and because it may provide quinol as substrate for redox driven energy transducing enzymes, it indirectly contributes to the build up of to the difference in transmembrane electrochemical potential [7,8] As a pyruvate oxidizing enzyme PQOs are hypothesized to play a role in bacterial carbon metabolism. In fact, in *Escherichia coli* (*E. coli*), this enzyme was shown to be able to support cell growth (in aerobic conditions) as an alternative to the pyruvate dehydrogenase multienzyme complex [9].

Despite early studies on this enzyme dating to the late 1950's and

* Corresponding author at: BioISI–Biosystems & Integrative Sciences Institute and Department of Chemistry and Biochemistry, Faculty of Sciences, University of Lisboa, 1749-016 Lisboa, Portugal.
E-mail address: mmpereira@fc.ul.pt (M.M. Pereira).

https://doi.org/10.1016/j.bbabio.2023.148958
Received 5 July 2022; Received in revised form 24 December 2022; Accepted 1 February 2023
Available online 7 February 2023

early 1960's [6,10,11], it has only been biochemically characterized from three different organisms: *E. coli*, *Corynebacterium glutamicum* (*C. glutamicum*) and *Staphylococcus aureus* (*S. aureus*). Currently, *E. coli*'s enzyme (the first PQO to be isolated and hence considered the "holotype" of this enzyme family) is known to be inactive in the cytoplasm due to the C-terminal blocking of the active site [6,12]. Pyruvate is oxidized by the TPP, which transfers the electrons to the FAD. This reduction is thought to induce structural changes on the protein leading to membrane recruitment through a lipid binding site at the C-terminal [4,13]. Upon membrane binding, a conformational rearrangement follows which exposes the active site and enhances the enzyme's activity by >20-fold [14–16]. The use of detergents and phospholipid membranes, or limited proteolysis of the C-terminal can replicate this effect in vitro [6].

The amount of structural information available on this enzyme family is still relatively scarce with the *E. coli*'s enzyme being the only example with an available crystallographic structure [5,6]. Some additional structural information has been inferred from comparison with PQO's soluble counterpart, the POX [17,18], that interacts with O_2, instead of the quinone, but further investigation on the amino acid sequence and structure/function of these monotopic enzymes is still needed. In this work we address this gap by investigating the amino acid sequence conservation of the PQO enzyme family as well as its taxonomic distribution. We evaluate the obtained results shedding light into the structure/function relationship of this enzyme family.

2. Materials and methods

KEGG's (Kyoto Encyclopedia of Genes and Genomes [19]) database was used to identify the studied PQO coding genes and access their respective presence/absence in genomes. PQO coding genes identification followed the workflow described in Fig. S1. Protein search was performed with pBLAST [20] (default parameters against all genomes deposited in KEGG's database, at April 2020) using the amino acid sequence of the PQO from *E. coli* (P07003 respective UniProt ID) as query. Results with an e-value of 0.01 or less were accepted for further analysis and manually filtered so that only one strain per species was included (ca. 8700 proteins). The complete information from each protein (amino acid sequence, UniProt ID, PDB ID and corresponding species name) was retrieved using a homemade python script. Selected protein sequences were clustered according to their identity using the CD-HIT tool [21] (50 % identity). The resulting 833 representative sequences were aligned using PROMALS3D (standard parameters), allowing to generate the Neighbour-Joining (NJ) dendrogram shown in Fig. S2. From the obtained dendrogram (visualized and manipulated in Dendroscope [22]), different TPP containing enzyme families were identified based on the distribution of the available crystallographic structures. Among these, the Pyruvate oxidase super-family could be separated from the remaining enzymes (red branch in Fig. S2). The dendrogram branch selected as containing pyruvate oxidases sequences included 56 items (clustered by >50 % identity), representatives of a dataset of 936 amino acid sequences. The 936 pyruvate oxidase sequences were reclustered with CD-HIT (90 % identity, 630 resulting sequences) and realigned with PROMALS3D to allow an accurate separation of the PQO and POX enzyme families (Fig. S3). PQO coding genes were identified based on 1) their corresponding KEGG annotation; 2) C-terminal extension; and 3) crystallographic structure distribution on the dendrogram of Fig. S3. The identified 469 PQO sequences were unclustered giving rise to a complete PQO dataset of 742 enzymes (Supplementary Excel File). These 742 amino acid sequences were aligned, a third and final time, using PROMALS3D, and were used to perform taxonomic profiling and sequence conservation analysis. Sequence conservation was calculated using JalView software [23]. Protein structural model visualization and figure construction were performed using PyMol [24]. *S. aureus*' PQO structure model was generated using PHYRE2 software [25], with *E. coli*'s PQO (PDB ID 3EY9) serving as template.

3. Taxonomic distribution

The presence of membrane bound pyruvate oxidases, PQOs, is already considered to be a prokaryotic exclusive feature. To further understand the taxonomic distribution of these enzymes we evaluated the presence of PQO coding genes in all species deposited in the KEGG's database. KEGG allows inferring not only the presence but also the absence of a specific coding gene, as it only contemplates fully sequenced genomes.

Our analysis revealed that, from the 6440 analysed genomes (corresponding to 3673 distinct species), 593 distinct species (~16 %) had at least one PQO coding gene (Fig. 2). From the identified genes, seven

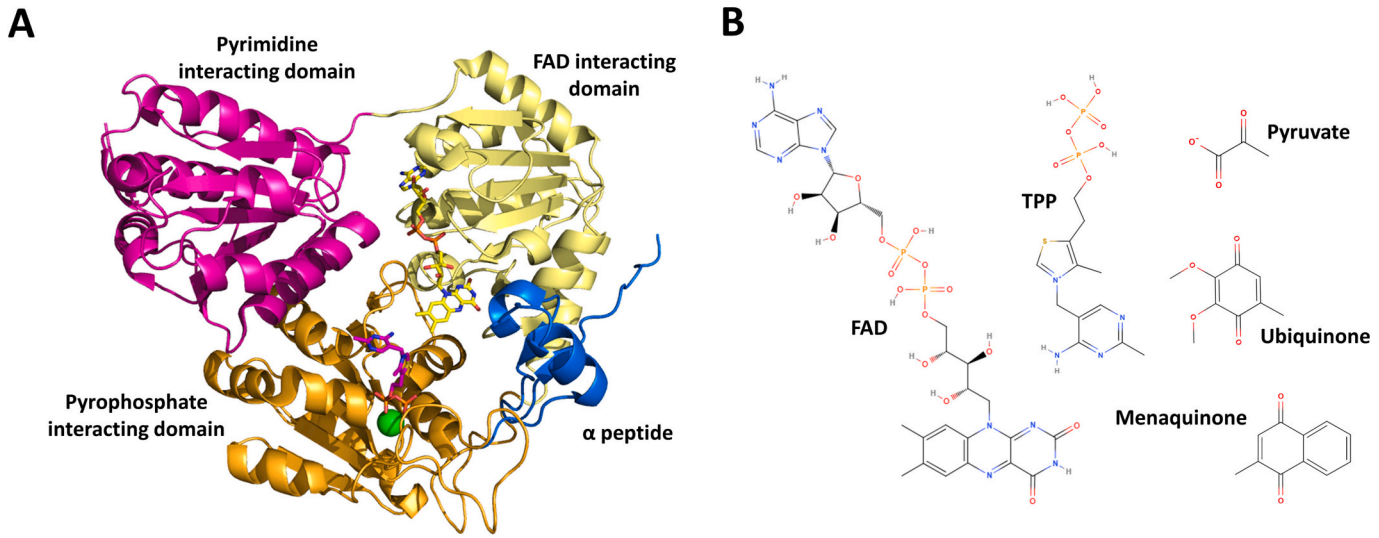

Fig. 1. *S. aureus* PQO structure model, substrates, and cofactors. A) Cartoon illustrating the structural domains of PQO: pyrimidine interacting domain (magenta), FAD interacting domain (yellow), pyrophosphate interacting domain (orange) and α-peptide (blue) (*E. coli*'s PQO (PDB ID 3EY9) was used as template for the generation of the shown template, using the PHYRE2 software. FAD is represented in yellow sticks, TPP in magenta sticks) and Mg^{2+} ion in green spheres. B) Chemical structures of the two PQO cofactors (FAD and TPP) and of the substrates: the electron donor (pyruvate) and the two possible electron acceptors (ubiquinone and menaquinone).

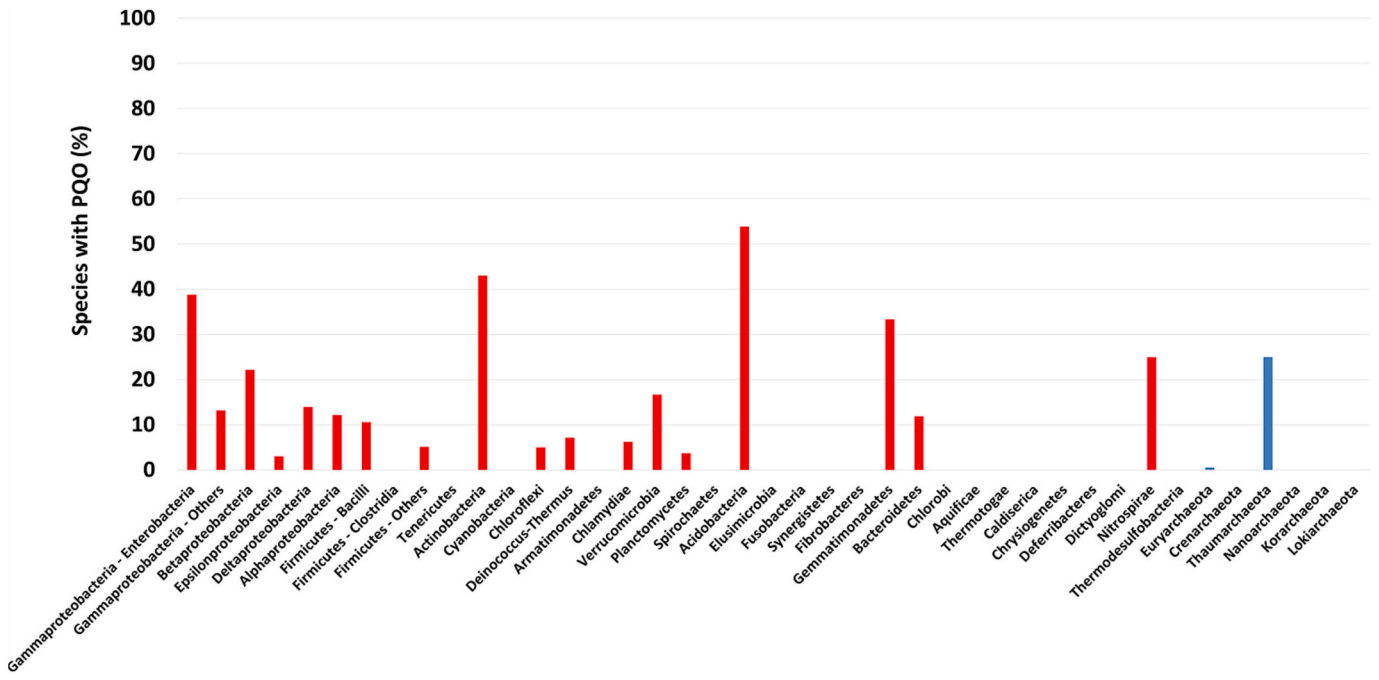

Fig. 2. PQO taxonomic distribution. Distribution of PQOs across Bacteria and Archaea phyla. Coloured bars indicate the percentage of species within a phylum with at least one PQO coding gene. The colour code is red for Bacteria and blue for Archaea.

belonged to Archaea and the remaining were Bacterial genes. These values correspond to 4 and 409 different species of Archaea and Bacteria respectively. Most notably this enzyme is absent from all eukaryotic organisms and from most Archaea (the exceptions here is one organism from the Euryarchaeota phylum (*Methanocella arvoryzae*, KEGG code: rci:RCIX1497) and three organisms from Nitrososphaera, a Thaumarchaeota specific genus; *Candidatus Nitrososphaera gargensis*, *Nitrososphaera viennensis*, *Candidatus Nitrososphaera evergladensis*; Respective KEGG codes: nga:Ngar_c26510, nvn:NVIE_000900 and nev:NTE_01425). In bacteria, the existence of a PQO coding gene is most common in Proteobacteria, Actinobacteria, Acidobacteria, Firmicutes, Bacteroidetes and some other less represented phyla (Table S1). The obtained taxonomic distribution seems to indicate no apparent relationship between the presence/absence of this enzyme and the type of respiratory metabolism, since we identified genes both in aerobic and anaerobic organisms. Contrarily, the harshness of the environment seems to coincide with the absence of PQO coding genes as no extremophilic organisms were retrieved in our analysis (illustrated by the absence of PQO coding genes in organisms as *Haloarcula marismortui*, *Deinococcus radiodurans*, *Methanopyrus kandleri* and *Picrophilus torridus*), despite this not being an exhaustive analysis. Some notable bacterial genus with PQO coding genes are: *Escherichia*, *Salmonella*, *Yersinia*, *Klebsiella*, *Pantoea*, *Xanthomonas*, *Pseudomonas*, *Burkholderia*, *Bradyrhizobium*, *Methylobacterium*, *Staphylococcus*, *Listeria*, *Mycobacterium* (curiously not *Mycobacterium tuberculosis*), *Corynebacterium*, *Nocardia*, *Gordonia* and *Streptomyces*.

PQOs from three organisms from distinct species have been successfully isolated and biochemically characterized. As previously mentioned in the introduction, the first PQO to be isolated and described was that from *E. coli* (UniProt ID: P07003) also known as PoxB [6,12]. The second PQO to be characterized was the one from *C. glutamicum* (UniProt ID: A0A1Q3DT68), being the first menaquinone reducing enzyme studied [3]. As PoxB the enzyme was shown to be activated by the presence of membrane mimicking agents and retain its activity in the pH range between 5.5 and 8.5. The enzyme was also shown to be able to use Mn^{2+} and Co^{2+} as cofactors for the binding of TPP [3]. More recently, the PQO from *S. aureus* (designated as CidC, UniProt ID: Q2FV86) was also isolated and characterized [26]. Contrarily to the previously studied PQOs, CidC was only slightly activated by phospholipid membranes or by equivalent proteolytic cleavage, suggesting the presence of different structural features. The enzyme was also a monomer around neutral pH, and active at more acidic pH possibly because of its decreased affinity for TPP around neutral pH values [26].

Examples of some PQO coding genes retrieved in this bioinformatic approach that have never been studied and that belong to potentially interesting organisms are those of: *Salmonella enterica* (UniProt ID: A0A0U0WGI0), *Yersinia pestis* (UniProt ID: A0A384KQ38), *Klebsiella pneumoniae* (UniProt ID: A6T6W9), *Pseudomonas aeruginosa* (UniProt IDs: Q9I207 and Q9HTQ7), *Bradyrhizobium japonicum* (UniProt ID: A0A1Y2JTG6) and *Burkholderia mallei* (UniProt ID: A0A0H2WBP4).

4. Conservation and structural hallmarks of PQOs

PQOs belong to the TPP containing enzymes super family [1], with each ~60 kDa monomer composed of four main domains: pyrimidine, pyrophosphate and FAD interacting domains, and the C-terminal domain. The dimeric conformation is believed to be essential for the mechanism of these enzymes, as the pyruvate catalytic site seems to be constituted by residues of the pyrimidine interacting domain of one subunit, and residues of the pyrophosphate interacting domain of the adjacent subunit [6].

Interestingly, *E. coli*'s PQO was found to adopt a homotetrameric form described as biologically relevant [6]. As all monotopic quinone reductases, PQOs are flavoproteins, harbouring a non-covalently bound FAD as a cofactor. The flavin, together with TPP are responsible for the oxidative decarboxylation of pyruvate and consequent electron transfer to the quinone.

To date, no sequence conservation study has been performed on the PQO protein family, despite the importance (conservation) of some residues being inferred from comparative studies with other TPP containing enzymes. By analysing the amino acid residue conservation profile of PQOs (Fig. 3), we observe that the regions of the enzyme with most conserved residues are the TPP and FAD binding regions, as well as the dimer interface region (Fig. S4).

From the roughly 570 residues within PQO's sequence, 105 were found to have a conservation over 80 % and 75 (out of these 105) over

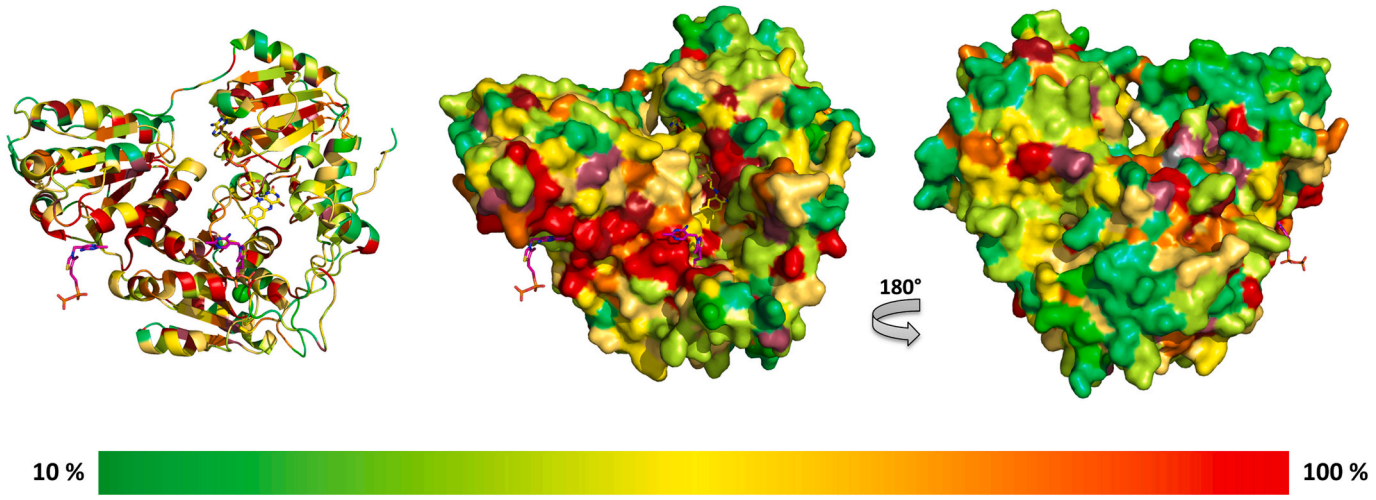

Fig. 3. Amino acid residue conservation heat-map of the PQO structure. Conservation from the least conserved regions to the most conserved regions is coloured in a green to red scale using *E. coli*'s PQO as template (PDB ID: 3EY9). FMN and TPP are represented in yellow and magenta sticks, respectively. Figure was built using Pymol.

90 % (Table S2). This sequence conservation study allowed us to search for functionally relevant conserved elements within the amino acid sequence of PQOs, confirming previously identified sequence motifs and exploring new structural hallmarks of these enzymes. The most significant observations are described below in more detail, always using *E. coli*'s PQO (UniProt ID: P07003) amino acid sequence as reference, with "*" indicating residues from a different monomer (Figs. 4, 5 and 6).

4.1. TPP binding

The TPP molecule may be separated into its thiamine and pyrophosphate moieties, each interacting with different domains of the PQO monomer. In both regions, the presence of highly conserved residues highlights the importance of the cofactor for the correct function of the enzyme (Fig. S5). The first line of conserved residues that directly interact with TPP is: G434 (100 %), N460 (100 %), L463 (97 %), E50* (100 %) and Q113* (99 %). A broader look into the TPP binding site allows to identify a second line of conserved residues that may also be relevant for the cofactor binding (not excluding their importance in other protein features): D379 (100 %), G381 (100 %), M408 (98 %), M438 (100 %), P76* (99 %), G77* (99 %). The exact role for all these residues is not known, as there is no biochemical data targeting most of them. Q113, for example, was proposed to interact with the hydroxyl group of lactyl-TPP (intermediate formed upon nucleophile attack of TPP to pyruvate), both in PQO and POX [6,27]. E50, a conserved glutamate throughout several TPP containing enzymes, interacts with N1 from the aminopyrimidine group, allowing the necessary aminopyrimidine-iminopyrimidine tautomerization for the reaction to proceed [28].

4.2. Mg^{2+} binding

PQOs were shown to be Mg^{2+} dependent enzymes. The magnesium ion binds to the pyrophosphate interacting domain of the enzyme and stabilizes TPP binding to PQO [26]. As frequently found in other enzymes [29,30], the Mg^{2+} ion has an octahedral coordination. In the case of PQOs this coordination is mediated by, besides the two TPP phosphates; the oxygen atoms of the side chains of N460 (100 %) and D433 (100 %); the oxygen of the main chain of V462 (30 %); and by a proximal water molecule (Fig. S6). With exception of V462 the atoms involved in the coordination of the metal ion are part of conserved PQO features expected to be found in all enzymes belonging to this family. The fact that X462 coordinates Mg^{2+} through its main chain, allows it not to be a fully conserved element with a residue distribution of 30 % serine, 29 % aspartate, 14 % valine, 10 % threonine, 5 % alanine and 12 % others.

4.3. FAD binding

As their soluble counterparts, PQOs have a non-covalently bound FAD to mediate the electron transfer from TPP to the electron acceptor (Fig. S5). The FAD interacting domain presents conserved residues, some of which are: i) those interacting with the isoalloxazine ring or the ribityl moiety, A233 (72 %), F276 (91 %), P277 (96 %), Y278 (90 %), F112* (61 %); ii) those interacting with the pyrophosphate region, G209 (100 %), L234 (83 %), S402 (99 %) and iii) those interacting with the adenine group, Q290 (98 %), D292 (98 %) and D311 (86 %). The cofactor binding role of most of the mentioned residues is largely understood, but for example in the cases of F276, Y278 and F112 (61 % phenylalanine, 31 % glutamine, 8 % other) they were proposed, in a study performed with POX, to interact with the *si* side of the isoalloxazine ring, forcing it to bend (possibly modulating its reactivity) [31]. In the same study, the authors identify a valine residue as responsible for stabilizing the FAD binding. Mutation of this residue to an alanine decreased the affinity and fold around the isoalloxazine ring without changing the kinetic properties of the enzyme. This valine residue present in POX seems to be absent from PQOs as in ~60 % of the cases a leucine is present (isoleucine in the remaining ~40 %, position 254 in *E. coli*'s PQO) [31].

4.4. HisGlu "dimer lock"

From our amino acid residue conservation analysis, combined with the available structural data, we were able to identify a highly conserved structural motif which we named "HEH lock" based on the residue composition of the motif, as it is composed of two histidine residues and one glutamate residue. The high conservation of these three residues H49 (90 %), E51 (99 %) and H80 (99 %) supports the idea of an important role for the enzyme's structure/function, as the presence of conserved charged/polar residues far from the solvent exposed surface, is linked to conformational specificity associated to molecular recognition and catalysis [32]. By analysing the structural position and arrangement of the HEH lock, it is tempting to speculate its role in the stabilization of the dimer interface. As Fig. S7 illustrates, the two histidine residues from one subunit (H49 and H80) interact with the glutamate residue from the opposing monomer (E50*), in this way forming a

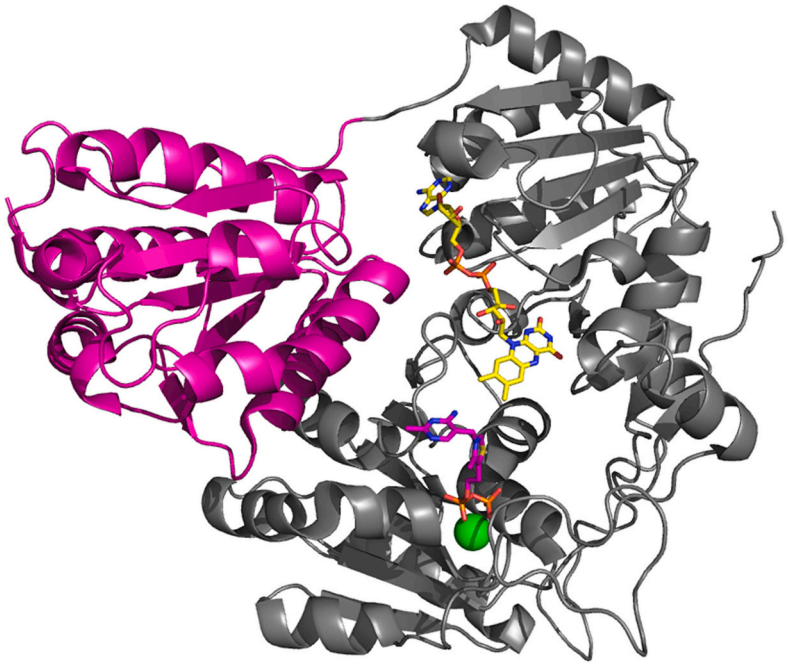

Fig. 4. PQO amino acid residue conservation of the pyrimidine binding domain. Cartoon represents the overall *E. coli*'s PQO structure (PDB ID 3EY9). Colour code: pyrimidine binding domain (magenta cartoon), the FAD in (yellow sticks), TPP (magenta sticks), protein main chain (grey cartoon), Mg^{2+} ion (green sphere). The table lists the amino acid residues present in at least 90 % of the identified PQO sequences (except for proline and glycine residues), as well as their conservation and proposed function.

***E. coli* PQO sequence**		**742 PQO sequences**		
Amino acid		Amino acid		Function
Number	Type	Conservation (%)	Consensus	
13	L	97	L	Structure/Fold
27	D	99	D	Pair with N30
30	N	93	N	Pair with D27
48	R	97	R	-
49	H	90	H	"HEH lock"
50	E	100	E	TPP binding
51	E	99	E	"HEH lock"
54	A	93	A	Structure/Fold
57	A	99	A	Structure/Fold
70	C	94	C	Structure/Fold
76	P	99	P	Pyruvate binding
80	H	99	H	"HEH lock"
81	L	93	L	Structure/Fold
85	L	93	L	Structure/Fold
87	D	93	D	Pair with S402
94	P	94	P	Structure/Fold
95	V	93	V	Structure/Fold
97	A	91	A	Structure/Fold
113	Q	99	Q	TPP binding
114	E	92	E	-
144	A	94	A	Structure/Fold
148	A	92	A	Structure/Fold
160	P	96	P	Structure/Fold
162	D	94	D	-

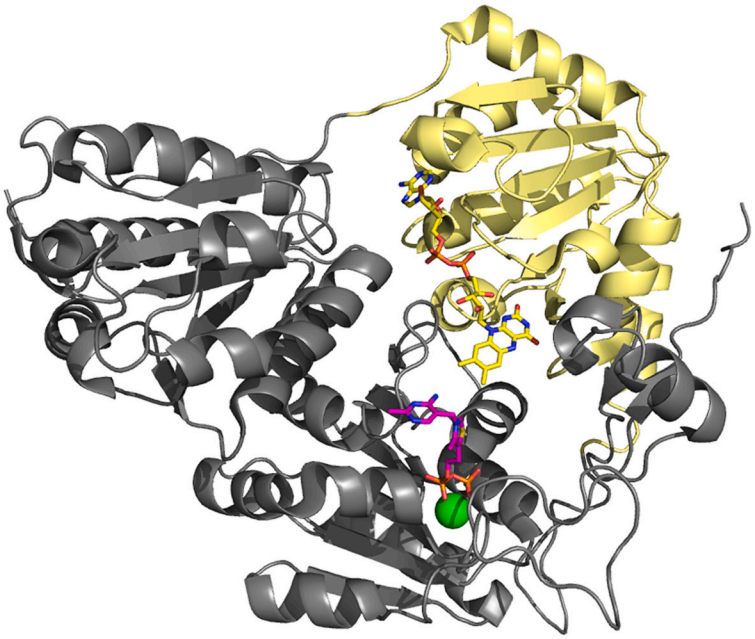

Fig. 5. PQO amino acid residue conservation of the FAD binding domain. Cartoon represents the overall *E. coli*'s PQO structure (PDB ID 3EY9). Colour code: FAD binding domain (pale yellow cartoon), the FAD in (yellow sticks), TPP (magenta sticks), protein main chain (grey cartoon), Mg^{2+} ion (green sphere). The table lists the amino acid residues present in at least 90 % of the identified PQO sequences (except for proline and glycine residues), as well as their conservation and proposed function.

***E. coli* PQO sequence**		**742 PQO sequences**		
Amino acid		Amino acid		Function
Number	Type	Conservation (%)	Consensus	
186	P	97	P	Structure/Fold
215	A	95	A	Structure/Fold
223	A	91	A	Structure/Fold
237	K	97	K	-
245	P	98	P	Structure/Fold
267	D	95	D	-
269	L	91	L	Structure/Fold
276	F	91	F	FAD ring interaction
277	P	96	P	Structure/Fold
278	Y	90	Y	FAD ring interaction
290	Q	98	Q	FAD binding
292	D	98	D	FAD binding
319	L	91	L	Structure/Fold

lock that seems to keep the dimer in place. In the roughly 10 % of the PQO sequences that do not have a histidine on position X49, an asparagine is present and expected to be able to functionally replace the lacking histidine. It is important to consider that this idea seems to be contradicted by the fact that *S. aureus*' PQO has the three residues composing the HEH lock but has been described as a monomer in solution [26]. Not excluding the possibility of these residues having distinct pKa's (influencing their protonation state and consequent electrostatics), another explanation for the role of this conserved feature is the regulation/stabilization of the previously mentioned E50, which is located right next to the HEH lock. In either case, further investigation focusing on these residues is needed.

4.5. α-Peptide

On the C-terminal region of PQO's structure, the α-peptide is located. This 20–25 amino acid region is known to play a key role in the functional attachment to the membrane. It was proposed that, when in solution, it blocks the active site, but upon flavin reduction it adopts a helical conformation mediating the recruitment of the protein to the membrane [4,13]. Despite its importance on the transition between active and inactive forms of the protein (membrane bound and soluble, respectively) no significantly conserved amino acid residues were found. The only noteworthy observation is the concentration of basic and positive residues in the α-peptide, which are likely to mediate the interaction with the negative charges of the lipid membrane: R552 (48 %), R558 (44 %), K567 (45 %), N569 (57 %), and R572 (27 %).

4.6. Other conserved residues

Some additional amino acid residues have been proposed to play important roles in the pyruvate oxidase family. F465 for example was proposed to intervein in the electron transfer between the thiamine and the flavin and on the expelling of the C-terminal region from the active site [6]. On our analysis F465 is only present in 43 % of the enzymes, with the remaining 57 % being mainly glutamine (27 %) and methionine

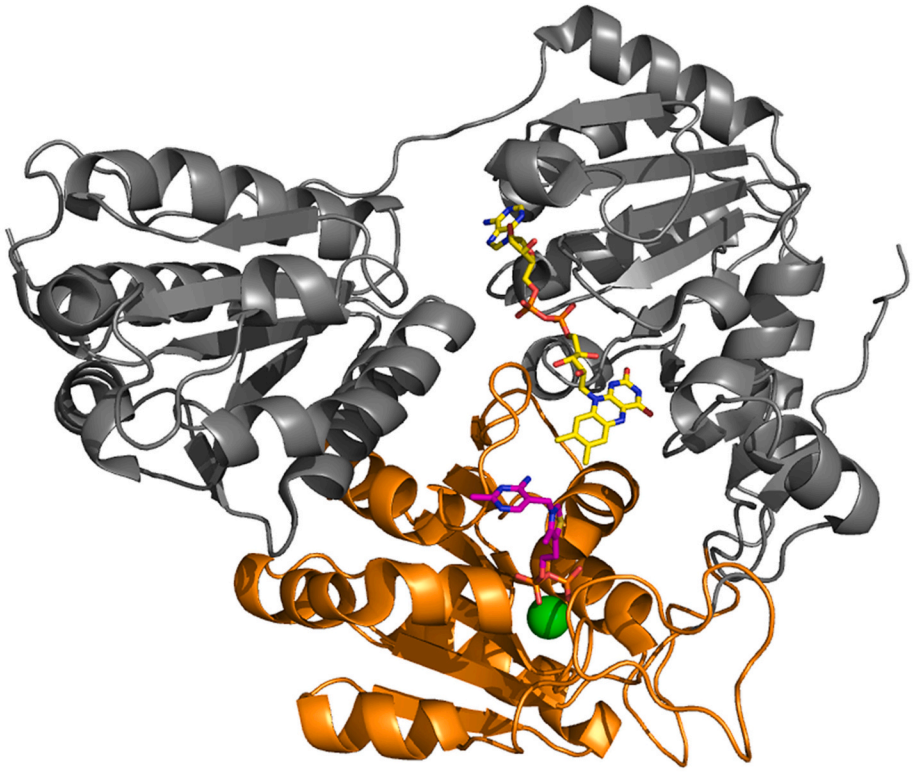

***E. coli* PQO sequence**		**742 PQO sequences**		
Amino acid		Amino acid		Function
Number	Type	Conservation (%)	Consensus	
359	P	98	P	Structure/Fold
379	D	100	D	-
386	W	97	W	-
389	R	97	R	-
402	S	99	S	Pair with D87
408	M	98	M	TPP binding
413	P	94	P	Structure/Fold
415	A	93	A	Structure/Fold
425	R	94	R	-
433	D	100	D	Mg^{2+} binding
438	M	100	M	TPP binding
460	N	100	N	Mg^{2+} binding
463	L	97	L	TPP binding
466	V	90	V	Structure/Fold
469	E	95	E	-
491	A	95	A	Structure/Fold
520	P	98	P	Structure/Fold

Fig. 6. PQO amino acid residue conservation of the pyrophosphate binding domain. Cartoon represents the overall *E. coli*'s PQO structure (PDB ID 3EY9). Colour code: pyrophosphate binding domain (orange cartoon), the FAD in (yellow sticks), TPP (magenta sticks), protein main chain (grey cartoon), Mg^{2+} ion (green sphere). The table lists the amino acid residues present in at least 90 % of the identified PQO sequences (except for proline and glycine residues), as well as their conservation and proposed function.

(25 %). This points to the possibility of other amino acid residues replacing this phenylalanine and occupying its side chain spatial position. In *Aerococcus viridans* pyruvate oxidase, L478 was proposed to function as a reaction lid, changing its conformation and consequent interaction with TPP [17,33]. In PQOs this, or an equivalent residue, does not exist. Instead D27 (99 %) and N30 (93 %) occupy that spatial region, suggesting they may perform a similar role in the membrane bound enzymes. Contrarily, a highly conserved residue for which no function has been proposed is D379 (100 %). In this case, the location of the residue (right between the two cofactors) leads to speculate a possible role in proton transfer or in structural changes signal propagation. As D379 other highly conserved residues in need of further experimental investigation and with no assigned function are W386 (97 %), R389 (97 %), R425 (94 %) and E469 (95 %).

5. Pyruvate metabolism and gene regulation of PQO

Organisms are constantly using their catabolism to metabolize energy rich molecules, such as glucose, to smaller metabolites. Glycolysis allows organisms to effectively oxidize glucose, leading to the build up of different intermediate molecules which can be used in different metabolic pathways according to the cell's needs. Arguably one of the most important molecules in catabolic metabolism is pyruvate, due to the number of biochemical pathways in which it participates (Fig. 7). Pyruvate is frequently presented as destined to follow one of four pathways leading to the formation of lactate, alanine, oxaloacetate, or acetyl-CoA. But in fact, pyruvate metabolism is considerably more diverse than this, as organisms have developed diverse ways of using pyruvate oxidation to produce a plethora of molecules, which are frequently overlooked. Despite being poorly explored, in terms of its cellular role, and considerably less ubiquitous than other pathways represented in Fig. 7, the oxidative decarboxylation of pyruvate is a

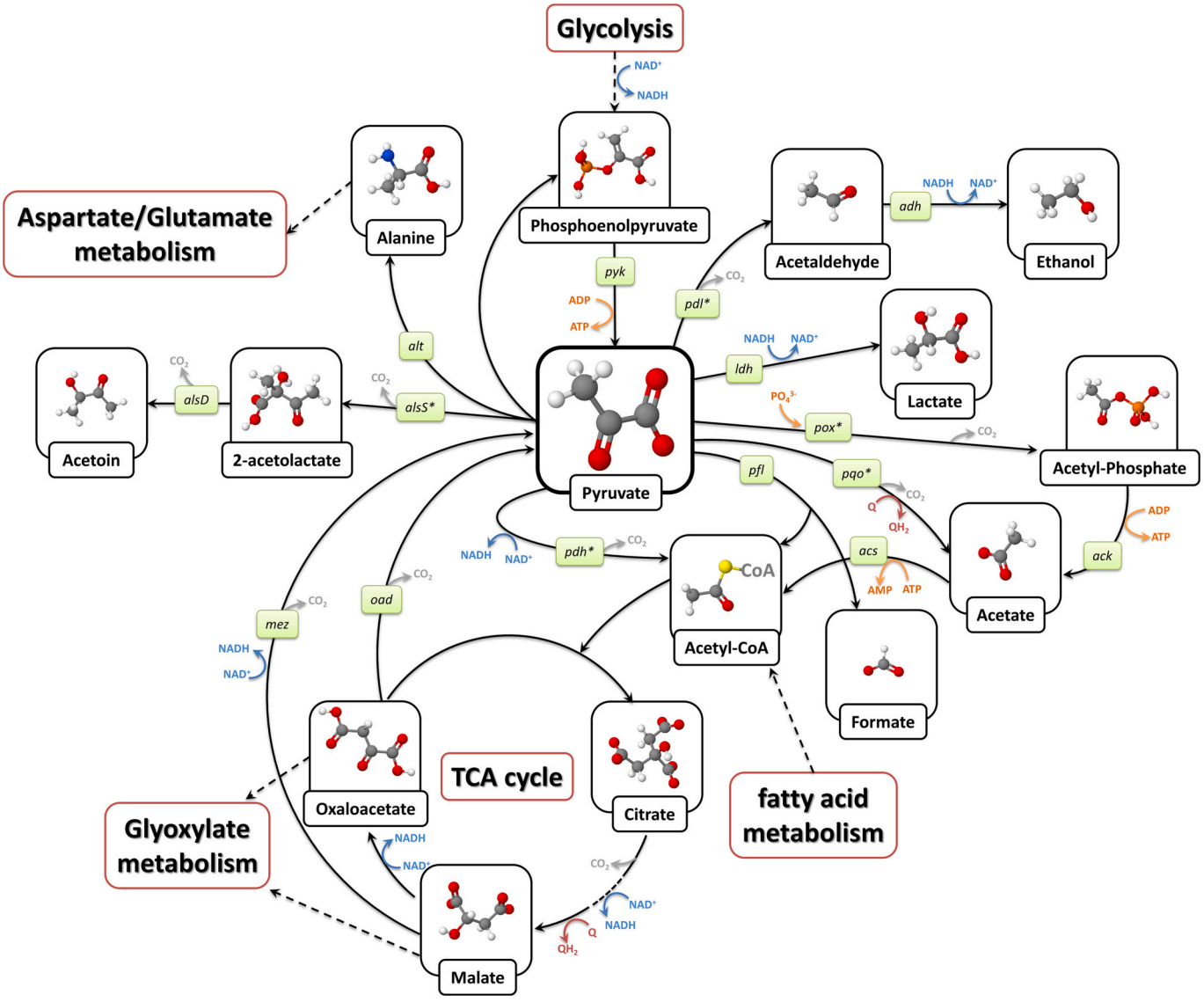

Fig. 7. Pyruvate related metabolism. Genes coding for proteins catalysing the illustrated reactions are coloured in green boxes: *pqo*, pyruvate:quinone oxidoreductase (EC 1.2.5.1); *pox*, pyruvate oxidase (EC 1.2.3.3); *pyk*, pyruvate kinase (EC 2.7.1.40); *mez*, malic enzyme (EC 1.1.1.39); *oad*, oxaloacetate decarboxylase (EC 4.1.1.3); *pdl*, pyruvate decarboxylase (EC 4.1.1.1); *pdh*, pyruvate dehydrogenase complex including E1, E2 and E3 subunits (EC 1.2.4.1); *alt*, alanine transaminase (EC 2.6.1.2); *ack*, acetate kinase (EC 2.7.2.1); *ldh* lactate dehydrogenase (EC 1.1.1.27); *adh*, alcohol dehydrogenase (EC 1.1.1.1); *alsS*, α-acetolactate synthase (EC 2.2.1.6); *alsD*, α-acetolactate decarboxylase (EC 4.1.1.5); *pfl*, pyruvate formate-lyase (EC 2.3.1.54); *acs*, acetyl-CoA synthethase (EC 6.2.2.1). Exact stoichiometry and additional reaction details are omitted for clarity. Genes marked with an "*" code for TPP containing enzymes.

possible biochemical process in organisms containing a PQO coding gene.

As an example, in *E. coli*, the pyruvate dehydrogenase complex ("pdh" in Fig. 7) and pyruvate formate-lyase ("pfl" in Fig. 7) oxidize pyruvate to acetyl-CoA during aerobic respiratory growth and fermentative growth, respectively [9]. This type of knowledge is still very scarce regarding PQO, but some information on the regulation of the corresponding coding genes from *S. aureus*, *E. coli*, and *C. glutamicum* may bring some light to the cellular role of pyruvate:quinone oxidoreductases.

E. coli's PQO coding gene (also known as *poxB*, "pqo" in Fig. 7) expression was found to be dependent on two stress regulators. RpoS, a sigma factor responsible for the transcription of several genes expressed at the end of the exponential phase and throughout the stationary phase during carbon stress conditions [34–37]; and SoxS, part of the SoxR/SoxS system, responsible for regulating the transcription of genes involved in adaptation to oxidative stress in *E. coli* [38]. PoxB coding gene was also shown to have an important role in the survival of cells growing under microaerobic conditions in which the pyruvate dehydrogenase complex and pyruvate formate lyase are not functioning properly [9,34]. PoxB was also proposed to function as an alternative in the response against oxidative stress resulting from a high metabolic flux through the pyruvate dehydrogenase complex (leading to the increase in NADH levels and consequent reactive oxygen species) [39]. Together, these results suggest that *poxB* may reach maximum expression levels during stationary growth phase, and that it participates in the regulated response to carbon and oxidative stresses.

S. aureus PQO coding gene (also known as *cidC*, "pqo" in Fig. 7) was found to be present in the cid operon alongside with the genes *cidA* and *cidB* [40–42]. This operon has been shown to be regulated by CidR [42,43], CcpA [44,45] and SrrB [46,47]. CidR directly regulates the *cidABC* operon as well as the alsSD operon, both involved in the catabolism of pyruvate [48]. As CidR expression depends on media acidification, its function was established as to limit acetate-mediated cell death in carbon rich conditions [49]. CcpA is the central transcription regulator of a mechanism used by Gram-positive bacteria to maximize their growth rate. This mechanism, known as carbon catabolite repression, represses the transcription of enzymes involved in the metabolism of less efficient carbon sources, prioritizing the catabolism of more advantageous ones [50,51]. Unlike induction of *cidABC* expression by CidR, regulation by CcpA requires fructose-1,6-biphosphate, an intermediate of glucose catabolism [45]. Expression of *cidABC* has also been shown to be repressed by the SrrAB system under conditions of excess of glucose, as a response to increased production of reactive oxygen species [46,47]. Generally, *cidC* expression seems to be induced upon media acidification or increase in glucose concentration, but it might be repressed in the presence of reactive oxygen species.

C. glutamicum PQO coding gene (also known as *pqo*, "pqo" in Fig. 7) is organized in an operon with two other downstream genes (*mapA* and *tipA*) which seem not to have any direct relationship with pyruvate metabolism. Studies with a *pqo* mutant strain revealed that the protein is not essential for *C. glutamicum* growth, and that it does not affect survival during stationary growth phase, or under phosphate starvation conditions [52]. Contrarily to the genes from *E. coli* and *S. aureus*, *C. glutamicum pqo* gene expression is independent on bacterial growth phase [52].

Overall, the regulation pathways of the PQO coding genes as well as the metabolic significance of the enzyme in the different organisms is still poorly understood, it seems that there is a significant divergence between different organisms, and that PQO function is highly variable from organism to organism.

6. Conclusion

In this work we performed the first thorough bioinformatics analysis applied to the PQO protein family. By using KEGG's database we were able to identify 742 PQO coding genes. Notably we did not retrieve any eukaryotic PQO coding gene, and we observed that most of these genes belong to Bacteria, with only seven of them belonging to Archaea. The presence of coding genes for this respiratory enzyme does not seem to be related with the type of respiration metabolism from the organism. PQOs are mainly present in Proteobacteria, Actinobacteria, Acidobacteria, Firmicutes and Bacteroidetes.

By identifying PQO coding genes we also performed a multiple sequence alignment to their corresponding amino acid sequences. By doing so, as we have done previously for other members of the monotopic quinone reductase super-family [53–55], we systematized the presence of structural/functional features among members of the PQO family. We found that out of the roughly 570 residues within PQO's sequence, 105 had a conservation over 80 % and 75 over 90 %. Not surprisingly, we also observed that most of those residues were located close to the cofactor binding sites. For most of the here identified as conserved residues there is no experimental biochemical data clarifying their role. One exception is for example Q113 (99 %), which is known to interact with TPP [6]. Our analysis allowed us to study the conservation of residues important for Mg^{2+}, TPP and FAD binding, as well as residues directly involved in the catalytic mechanism. Interestingly, we did not find any conserved residues in the protein region corresponding to the α-peptide (C-terminal region responsible for membrane interaction), suggesting that membrane interaction is governed by unspecific interactions, such as electrostatic ones. We also established the presence of a new conserved structural feature, represented by the a "HEH" motif, expected to be involved in the dimerization process, due to its structure location.

We finalized this work by reviewing the existing data regarding PQO coding genes regulation, relating it with the cellular function of the enzyme. PQOs are hypothesized as alternatives to the canonical pyruvate catabolizing enzymes. We found out that in some cases gene expression is dependent on glucose concentration, medium acidification, or reactive oxygen species accumulation, but this is not always the case, suggesting that PQO cellular function may vary from organism to organism. The results described in this work not only contribute to a better understanding of the biochemistry of these respiratory proteins, but also to the broader family of TPP containing enzymes. They will also ignite further investigation targeting the conserved structural features that were here established.

Declaration of competing interest

The authors declare that they have no known competing financial interests or personal relationships that could have appeared to influence the work reported in this paper.

Data availability

Data will be made available on request.

Acknowledgements

FMS is recipient of fellowship by Fundação para a Ciência e a Tecnologia (PD/BD/128213/2016, within the scope of the PhD program Molecular Biosciences PD/00133/2012). The work was funded by Fundação para a Ciência e a Tecnologia (PTDC/BIA-BQM/2599/2021). The project was supported by UIDB/04046/2020 and UIDP/04046/2020 Centre grants from FCT, Portugal (to BioISI), by LISBOA-01-0145-FEDER-007660 co-funded by FEDER through COMPETE2020-POCI.

Appendix A. Supplementary data

Supplementary data to this article can be found online at https://doi.org/10.1016/j.bbabio.2023.148958.

References

[1] R.G. Duggleby, Domain relationships in thiamine diphosphate-dependent enzymes, Acc. Chem. Res. 39 (2006) 550–557, https://doi.org/10.1021/ar068022z.

[2] R.B. Gennis, L.P. Hager, Pyruvate oxidase, in: Enzym. Bioligical Membr, Springer US, Boston, MA, 1976, pp. 493–504, https://doi.org/10.1007/978-1-4684-2655-7_14.

[3] M.E. Schreiner, B.J. Eikmanns, Pyruvate:quinone oxidoreductase from corynebacterium glutamicum: purification and biochemical characterization, J. Bacteriol. 187 (2005) 862–871, https://doi.org/10.1128/JB.187.3.862-871.2005.

[4] M.W. Mather, R.B. Gennis, Spectroscopic studies of pyruvate oxidase flavoprotein from Escherichia coli trapped in the lipid-activated form by cross-linking, J. Biol. Chem. 260 (1985) 10395–10397, https://doi.org/10.1016/s0021-9258(19)85094-9.

[5] A. Weidner, P. Neumann, G. Wille, M.T. Stubbs, K. Tittmann, Crystallization and preliminary X-ray diffraction analysis of full-length and proteolytically activated pyruvate oxidase from Escherichia coli, Acta Crystallogr. Sect. F. Struct. Biol. Cryst. Commun. 64 (2008) 179–181, https://doi.org/10.1107/S1744309108003473.

[6] P. Neumann, A. Weidner, A. Pech, M.T. Stubbs, K. Tittmann, Structural basis for membrane binding and catalytic activation of the peripheral membrane enzyme pyruvate oxidase from Escherichia coli, Proc. Natl. Acad. Sci. 105 (2008) 17390–17395, https://doi.org/10.1073/pnas.0805027105.

[7] P.N. Refojo, F.V. Sena, F. Calisto, F.M. Sousa, M.M. Pereira, The plethora of membrane respiratory chains in the phyla of life, in: Adv. Microb. Physiol, Academic Press, 2019, pp. 331–414, https://doi.org/10.1016/bs.ampbs.2019.03.002.

[8] B.C. Marreiros, F. Calisto, P.J. Castro, A.M. Duarte, F.V. Sena, A.F. Silva, F. M. Sousa, M. Teixeira, P.N. Refojo, M.M. Pereira, Exploring membrane respiratory chains, Biochim. Biophys. Acta - Bioenerg. 2016 (1857) 1039–1067, https://doi.org/10.1016/j.bbabio.2016.03.028.

[9] A.M. Abdel-Hamid, M.M. Attwood, J.R. Guest, Pyruvate oxidase contributes to the aerobic growth efficiency of Escherichia coli, Microbiology 147 (2001) 1483–1498, https://doi.org/10.1099/00221287-147-6-1483.

[10] S.S. Deeb, L.P. Hager, Crystaline cytochrome b1 from Escherichia coli, J. Biol. Chem. 239 (1964) 1024–1031. http://www.ncbi.nlm.nih.gov/pubmed/14165901.

[11] L.P. Hager, Activation of a ferricyanide linked pyruvate oxidase by α-tocopherol esters, J. Am. Chem. Soc. 79 (1957) 5575–5576, https://doi.org/10.1021/ja01577a064.

[12] M.A. Recny, L.P. Hager, Isolation and characterization of the protease-activated form of pyruvate oxidase. Evidence for a conformational change in the environment of the flavin prosthetic group, J. Biol. Chem. 258 (1983) 5189–5195. http://www.ncbi.nlm.nih.gov/pubmed/6339508.

[13] M.A. Recny, L.P. Hager, Isolation and characterization of the protease-activated form of pyruvate oxidase. Evidence for a conformational change in the environment of the flavin prosthetic group, J. Biol. Chem. 258 (1983) 5189–5195, https://doi.org/10.1016/S0021-9258(18)32557-2.

[14] R. Blake, L.P. Hager, Activation of pyruvate oxidase by monomeric and micellar amphiphiles, J. Biol. Chem. 253 (1978) 1963–1971. http://www.ncbi.nlm.nih.gov/pubmed/632248.

[15] S.E. Hamilton, M. Recny, L.P. Hager, Identification of the high-affinity lipid binding site in Escherichia coli pyruvate oxidase, Biochemistry 25 (1986) 8178–8183, https://doi.org/10.1021/bi00373a009.

[16] Y.Y. Chang, J.E. Cronan, An Escherichia coli mutant deficient in pyruvate oxidase activity due to altered phospholipid activation of the enzyme, Proc. Natl. Acad. Sci. U. S. A. 81 (1984) 4348–4352, https://doi.org/10.1073/pnas.81.14.4348.

[17] E.C.M. Juan, M.M. Hoque, M.T. Hossain, T. Yamamoto, S. Imamura, K. Suzuki, T. Sekiguchi, A. Takénaka, The structures of pyruvate oxidase from aerococcus viridans with cofactors and with a reaction intermediate reveal the flexibility of the active-site tunnel for catalysis., acta crystallogr, Sect. F. Struct. Biol. Cryst. Commun. 63 (2007) 900–907, https://doi.org/10.1107/S1744309107041012.

[18] Y.A. Muller, G. Schumacher, R. Rudolph, G.E. Schulz, The refined structures of a stabilized mutant and of wild-type pyruvate oxidase from lactobacillus plantarum, J. Mol. Biol. 237 (1994) 315–335, https://doi.org/10.1006/jmbi.1994.1233.

[19] H. Ogata, S. Goto, K. Sato, W. Fujibuchi, H. Bono, M. Kanehisa, KEGG: Kyoto encyclopedia of genes and genomes, Nucleic Acids Res. (1999), https://doi.org/10.1093/nar/27.1.29.

[20] S.F. Altschul, W. Gish, W. Miller, E.W. Myers, D.J. Lipman, Basic local alignment search tool, J. Mol. Biol. (1990), https://doi.org/10.1016/S0022-2836(05)80360-2.

[21] Y. Huang, B. Niu, Y. Gao, L. Fu, W. Li, CD-HIT suite: a web server for clustering and comparing biological sequences, Bioinformatics (2010), https://doi.org/10.1093/bioinformatics/btq003.

[22] D.H. Huson, D.C. Richter, C. Rausch, T. Dezulian, M. Franz, R. Rupp, Dendroscope: an interactive viewer for large phylogenetic trees, BMC Bioinformatics (2007), https://doi.org/10.1186/1471-2105-8-460.

[23] A.M. Waterhouse, J.B. Procter, D.M.A. Martin, M. Clamp, G.J. Barton, Jalview version 2-a multiple sequence alignment editor and analysis workbench, Bioinformatics (2009), https://doi.org/10.1093/bioinformatics/btp033.

[24] L. Schrödinger, The PyMol Molecular Graphics System, Versión 1.8, Thomas Hold, 2015, https://doi.org/10.1007/s13398-014-0173-7.2.

[25] L.A. Kelley, S. Mezulis, C.M. Yates, N.W. Mark, M.J. Sternberg, The Phyre2 web portal for protein modeling, prediction and analysis, Nat. Protoc. 10 (2015) 845–858.

[26] X. Zhang, K.W. Bayles, S. Luca, Staphylococcus aureus CidC is a pyruvate: menaquinone oxidoreductase, Biochemistry 56 (2017) 4819–4829, https://doi.org/10.1021/acs.biochem.7b00570.

[27] P.A. Frey, Snapshots of three intermediates at the active site of pyruvate oxidase, Nat. Chem. Biol. 2 (2006) 294–295, https://doi.org/10.1038/nchembio0606-294.

[28] A. Kaplun, E. Binshtein, M. Vyazmensky, A. Steinmetz, Z. Barak, D.M. Chipman, K. Tittmann, B. Shaanan, Glyoxylate carboligase lacks the canonical active site glutamate of thiamine-dependent enzymes, Nat. Chem. Biol. 4 (2008) 113–118, https://doi.org/10.1038/nchembio.62.

[29] Z. Zhao, Z. Ma, B. Wang, Y. Guan, X.-D. Su, Z. Jiang, Mn2+ directly activates cGAS and structural analysis suggests Mn2+ induces a noncanonical catalytic synthesis of 2′3′-cGAMP, Cell Rep. 32 (2020), 108053, https://doi.org/10.1016/j.celrep.2020.108053.

[30] R. Bonn-Breach, Y. Gu, J. Jenkins, R. Fasan, J. Wedekind, Structure of sonic hedgehog protein in complex with zinc(II) and magnesium(II) reveals ion-coordination plasticity relevant to peptide drug design, acta crystallogrSect. D, Struct. Biol. 75 (2019) 969–979, https://doi.org/10.1107/S2059798319012890.

[31] G. Wille, M. Ritter, M.S. Weiss, S. König, W. Mäntele, G. Hübner, The role of Val-265 for flavin adenine dinucleotide (FAD) binding in pyruvate oxidase: FTIR, kinetic, and crystallographic studies on the enzyme variant V265A, Biochemistry 44 (2005) 5086–5094, https://doi.org/10.1021/bi047337o.

[32] J.E. Donald, D.W. Kulp, W.F. DeGrado, Salt bridges: geometrically specific, designable interactions, Proteins Struct. Funct. Bioinform. 79 (2011) 898–915, https://doi.org/10.1002/prot.22927.

[33] K. Tittmann, R. Golbik, K. Uhlemann, L. Khailova, G. Schneider, M. Patel, F. Jordan, D.M. Chipman, R.G. Duggleby, G. Hübner, NMR analysis of covalent intermediates in thiamin diphosphate enzymes †, Biochemistry 42 (2003) 7885–7891, https://doi.org/10.1021/bi034465o.

[34] Y.Y. Chang, A.Y. Wang, J.E. Cronan, Expression of Escherichia coli pyruvate oxidase (PoxB) depends on the sigma factor encoded by the rpoS(katF) gene, Mol. Microbiol. 11 (1994) 1019–1028, https://doi.org/10.1111/j.1365-2958.1994.tb00380.x.

[35] R. Hengge-Aronis, Signal transduction and regulatory mechanisms involved in control of the σS (RpoS) subunit of RNA polymerase, Microbiol. Mol. Biol. Rev. 66 (2002) 373–395, https://doi.org/10.1128/MMBR.66.3.373-395.2002.

[36] L. Notley, T. Ferenci, Induction of RpoS-dependent functions in glucose-limited continuous culture: what level of nutrient limitation induces the stationary phase of Escherichia coli? J. Bacteriol. 178 (1996) 1465–1468, https://doi.org/10.1128/JB.178.5.1465-1468.1996.

[37] S.R.V. Vijayakumar, M.G. Kirchhof, C.L. Patten, H.E. Schellhorn, RpoS-regulated genes of Escherichia coli identified by random lacZ fusion mutagenesis, J. Bacteriol. 186 (2004) 8499–8507, https://doi.org/10.1128/JB.186.24.8499-8507.2004.

[38] N. Flores, R. de Anda, S. Flores, A. Escalante, G. Hernández, A. Martínez, O. T. Ramírez, G. Gosset, F. Bolívar, Role of pyruvate oxidase in Escherichia coli strains lacking the phosphoenolpyruvate:carbohydrate phosphotransferase system, J. Mol. Microbiol. Biotechnol. 8 (2004) 209–221, https://doi.org/10.1159/000086702.

[39] P.L. Moreau, Diversion of the metabolic flux from pyruvate dehydrogenase to pyruvate oxidase decreases oxidative stress during glucose metabolism in nongrowing Escherichia coli cells incubated under aerobic, phosphate starvation conditions, J. Bacteriol. 186 (2004) 7364–7368, https://doi.org/10.1128/JB.186.21.7364-7368.2004.

[40] K.C. Rice, B.A. Firek, J.B. Nelson, S.-J. Yang, T.G. Patton, K.W. Bayles, The Staphylococcus aureus cidAB operon: evaluation of its role in regulation of murein hydrolase activity and penicillin tolerance, J. Bacteriol. 185 (2003) 2635–2643, https://doi.org/10.1128/jb.185.8.2635-2643.2003.

[41] K.C. Rice, T. Patton, S.-J. Yang, A. Dumoulin, M. Bischoff, K.W. Bayles, Transcription of the Staphylococcus aureus cid and lrg murein hydrolase regulators is affected by sigma factor B, J. Bacteriol. 186 (2004) 3029–3037, https://doi.org/10.1128/JB.186.10.3029-3037.2004.

[42] K.C. Rice, J.B. Nelson, T.G. Patton, S.-J. Yang, K.W. Bayles, Acetic acid induces expression of the Staphylococcus aureus cidABC and lrgAB murein hydrolase regulator operons, J. Bacteriol. 187 (2005) 813–821, https://doi.org/10.1128/JB.187.3.813-821.2005.

[43] S.-J. Yang, K.C. Rice, R.J. Brown, T.G. Patton, L.E. Liou, Y.H. Park, K.W. Bayles, A LysR-type regulator, CidR, is required for induction of the Staphylococcus aureus cidABC operon, J. Bacteriol. 187 (2005) 5893–5900, https://doi.org/10.1128/JB.187.17.5893-5900.2005.

[44] K. Seidl, C. Goerke, C. Wolz, D. Mack, B. Berger-Bächi, M. Bischoff, Staphylococcus aureus CcpA affects biofilm formation, Infect. Immun. 76 (2008) 2044–2050, https://doi.org/10.1128/IAI.00035-08.

[45] M.R. Sadykov, I.H. Windham, T.J. Widhelm, V.K. Yajjala, S.M. Watson, J.L. Endres, A.I. Bavari, V.C. Thomas, J.L. Bose, K.W. Bayles, CidR and CcpA synergistically regulate Staphylococcus aureus cidABC expression, J. Bacteriol. 201 (2019), https://doi.org/10.1128/JB.00371-19.

[46] I.H. Windham, S.S. Chaudhari, J.L. Bose, V.C. Thomas, K.W. Bayles, SrrAB modulates Staphylococcus aureus cell death through regulation of cidABC transcription, J. Bacteriol. 198 (2016) 1114–1122, https://doi.org/10.1128/JB.00954-15.

[47] J.M. Yarwood, J.K. McCormick, P.M. Schlievert, Identification of a novel two-component regulatory system that acts in global regulation of virulence factors of Staphylococcus aureus, J. Bacteriol. 183 (2001) 1113–1123, https://doi.org/10.1128/JB.183.4.1113-1123.2001.

[48] S.-J. Yang, P.M. Dunman, S.J. Projan, K.W. Bayles, Characterization of the Staphylococcus aureus CidR regulon: elucidation of a novel role for acetoin

metabolism in cell death and lysis, Mol. Microbiol. 60 (2006) 458–468, https://doi.org/10.1111/j.1365-2958.2006.05105.x.
[49] S.S. Chaudhari, V.C. Thomas, M.R. Sadykov, J.L. Bose, D.J. Ahn, M.C. Zimmerman, K.W. Bayles, The LysR-type transcriptional regulator, CidR, regulates stationary phase cell death in Staphylococcus aureus, Mol. Microbiol. 101 (2016) 942–953, https://doi.org/10.1111/mmi.13433.
[50] J. Stülke, W. Hillen, Regulation of carbon catabolism in bacillus species, Annu. Rev. Microbiol. 54 (2000) 849–880, https://doi.org/10.1146/annurev.micro.54.1.849.
[51] R. Brückner, F. Titgemeyer, Carbon catabolite repression in bacteria: choice of the carbon source and autoregulatory limitation of sugar utilization, FEMS Microbiol. Lett. 209 (2002) 141–148, https://doi.org/10.1111/j.1574-6968.2002.tb11123.x.
[52] M.E. Schreiner, C. Riedel, J. Holátko, M. Pátek, B.J. Eikmanns, Pyruvate: quinone oxidoreductase in corynebacterium glutamicum: molecular analysis of the pqo gene, significance of the enzyme, and phylogenetic aspects, J. Bacteriol. 188 (2006) 1341–1350, https://doi.org/10.1128/JB.188.4.1341-1350.2006.
[53] F.M. Sousa, J.G. Pereira, B.C. Marreiros, M.M. Pereira, Taxonomic distribution, structure/function relationship and metabolic context of the two families of sulfide dehydrogenases: SQR and FCSD, Biochim. Biophys. Acta - Bioenerg. 1859 (2018), https://doi.org/10.1016/j.bbabio.2018.04.004.
[54] F.M. Sousa, P.N. Refojo, M.M. Pereira, Investigating the amino acid sequences of membrane bound dihydroorotate:quinone oxidoreductases (DHOQOs): structural and functional implications, Biochim. Biophys. Acta - Bioenerg. 1862 (2021), https://doi.org/10.1016/j.bbabio.2020.148321.
[55] B.C. Marreiros, F.V. Sena, F.M. Sousa, A.P. Batista, M.M. Pereira, N.A.D.H. Type II, Quinone oxidoreductase family: phylogenetic distribution, structural diversity and evolutionary divergences, Environ. Microbiol. 00 (2016), https://doi.org/10.1111/1462-2920.13352.